



Modelling and Optimization Combined Heat and Power with Photovoltaic/Thermal system

Reza Alayi^{1, 2, *}, Yaser Ebazadeh³, Mehdi Jahangiri^{2, *}

¹Department of Mechanics, Germi Branch, Islamic Azad University, Germi, Iran, Reza_Alayi@iau.ac.ir

²Energy Research Center, Shahrekord Branch, Islamic Azad University, Shahrekord, Iran, Mehdi_Jahangiri@yahoo.com

³Department of Computer Engineering, Germi Branch, Islamic Azad University, Germi, Iran, yaser.ebazadeh@iau.ac.ir

Abstract

In the present study, the aim is to model and optimize the photovoltaic/thermal system (PVT) to achieve the highest thermal and electrical efficiencies by considering the physical characteristics. To model the proposed system, the governing relations were derived by considering the desired variables. Then to use the modeling, the validation of the code was done with a valid source, for which the variables of cell surface temperature, a bottom surface, and output fluid were used. After validation, it was observed that the proposed model has good accuracy to achieve the desired goals. To achieve maximum output power by the cell, open circuit voltage and short circuit current for this system was calculated for one day that has the highest radiation intensity, for which the highest voltage and current are 9.3 V and 6.7 A, respectively. Then, after extraction of voltage and short circuit current for the studied cell, the amount of thermal and electrical efficiencies was determined to be 40% and 10%, respectively. In the next step of this research, optimization is performed to achieve the highest efficiency, which is 67% for this system.

Keywords: Modeling, Optimization, Photovoltaic/thermal, Thermal and electrical efficiencies.

Article history: Received 2023/03/13; Revised 2023/05/14; Accepted 2023/05/14, Article Type: Research paper

© 2023 IAUCTB-IJSEE Science. All rights reserved

<https://doi.org/10.30495/ijsee.2023.1981667.1257>

1. Introduction

Due to the importance of using renewable energy sources in the energy supply, the use of these resources is increasing rapidly [1-3]. Also due to the emission of pollutants from combustion, increase in carbon dioxide in the atmosphere, rising temperatures, climate change, rising sea levels, and a sharp decline in fuels such as oil, coal, and non-renewable existence of these fuels [4, 5], the production of renewable energy such as wind and solar has become very important and the use of this type of energy to provide the necessary power to produce electrical and thermal power has been studied [6, 7]. One of the renewable energies is solar energy, which is widely available to everyone [8, 9]. The most common technology for using solar energy is the use of photovoltaic cells [10-12]. In a standard module, most of the radiation from the sun is converted into heat by photovoltaic cells, which is lost in exchange with the environment, and a small part of the radiation reaching the cells is converted

into electrical energy and this heat production increases the temperature of the cell surface and thus reduces the efficiency of the cell [13, 14]. The output power is inversely proportional to the cell surface temperature. In other words, with increasing temperature, the output voltage decreases. As a result, increasing the temperature reduces the open circuit voltage and output power of the cell. In most silicon cells, the output power decreases by about 0.5% per degree of temperature rise [15, 16]. Therefore, for the electrical efficiency of the cell to remain constant, the heat generated on the cell surface must be expelled. Fluid flow around the photovoltaic panels can be used to dissipate the heat generated during the photon collision with the cell surface [17-19]. By moving the fluid through the panel, a large part of this heat can be absorbed from the panel, which reduces the surface temperature and thus increases the electrical efficiency [20, 21]. The PVT systems can collect solar energy at

different wavelengths, thus increasing energy efficiency and exergy [22, 23]. It is a combination of photovoltaics and solar heating and some of the studies that have been done in this regard are discussed below.

On the other hand, Fayaz et al. [11] have done research entitled Numerical and outdoor real-time experimental investigation of the performance of PCM-based PVT system, the purpose of this study is to the effect of radiation intensity on the heat produced. In 2019, Fudholi et al. A theoretical and laboratory study of thermal photovoltaics has been performed. After modeling, exergy analysis has been performed to achieve high thermal efficiency.

In this study, the air is assumed for cell cooling [12]. In the same year, Herrando et al. have done research entitled Solar combined cooling, heating, and power systems based on hybrid PVT, PV, or solar-thermal collectors for building applications [29].

In this research, an attempt has been made to determine the variables such as the response rate of the system to the electric load, the amount of electrical energy produced, the amount of investment cost, and the rate of return on investment from many variables that can be in this project. By specifying the above variables, the system can be compared with common systems used in industry, and important results can be achieved.

Table.1.
Some research on the combination of photovoltaics and solar heating

Reference	Location	Solar Technology	Working Fluid	Result
[24]	Malaysia	PVT	Water	The solar system is a suitable complement to the heat pump
[25]	Iran	PVT	Air	Thermal and electrical efficiencies are inversely related
[26]	Denmark	PVT	Air	Variability of electrical and thermal efficiencies relative to solar radiation
[27]	Korea	PVT	Water	Check the cover tube on the efficiency PVT
[28]	Iran	PVT	Water	The direct effect of physical characteristics on efficiency

2. Materials and methods

A) Modeling PVT system

The system studied in this research is a PVT collector consisting of two layers: a glazed or non-freezing PV layer above and below it, and an absorption layer that absorbs heat from the PV layer. The absorption layer has inlets and outlets for fluid circulation. Liquid, which may be liquid (such as a mixture of water or water of ethylene glycol) or air, passes through the adsorbed substance to extract heat. The following is the working mechanism of a sample PV/T collector:

As shown in Figure 1, when solar radiation hits the cell surface, electrical energy is generated, and accordingly, the temperature of the cell surface increases, which is absorbed by the fluid with the flow of fluid in the underlying layers of the cell, and thermal energy is produced. Using a water-ethylene-glycol mixture instead of water can prevent the liquid from freezing at cold temperatures and thus protect the collector from deformation problems due to freezing.

B) Thermal analysis

For the sake of brevity, the proof of the relations governing thermal performance is avoided. In these equations, most of the parameters that PV/T can be changed are assumed to be variables. Figure 2 shows the equivalent thermal resistance circuit and PV/T schematic cross-section of the flow duct.

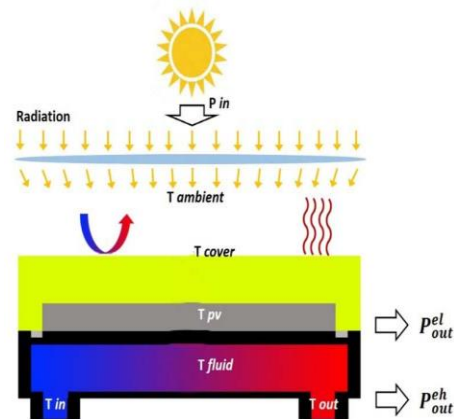


Fig. 1. The PVT schematic [12]

By applying the energy balance for the various components of the PVT system, its thermal efficiency is obtained. The energy balance for the cell modulus can be expressed according to Equation 1 [28, 29].

$$\begin{aligned} \tau_G[\alpha_c\beta_cG + \alpha_T(1 - \beta_c)G]bdx \\ = \tau_G\beta_c\eta_{el}Gbdx \\ + [U_t(T_{cell} - T_{amb}) \\ + U_T(T_{cell} - T_{bs})]bdx \end{aligned} \quad (1)$$

The heat transfer coefficient from the photovoltaic cell to the fluid flow through the Tedlar (U_T) can be calculated as Equation 2 [28, 29]:

$$U_T = [L_T/K_T + L_i/K_i]^{-1} \quad (2)$$

The total heat transfer coefficient of the solar cell to the environment through PV/T glass coating (U_t) can be calculated as Equation 3 [24, 25]:

$$U_t = [L_G/K_G + 1/h_{conv,t} + 1/h_{rad}]^{-1} \quad (3)$$

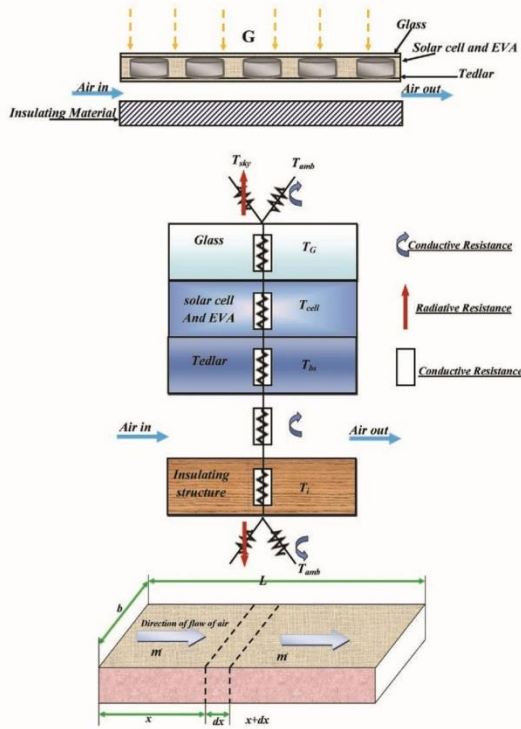


Fig. 2. Equivalent thermal resistance circuit and cross-section of the flow duct of PVT

The heat transfer coefficient of displacement from the upper surface of PV/T to the environment for surfaces in a horizontal position can be calculated by Equation 4.

$$h_{conv,t} = 2.8 + 3V_w \quad (4)$$

The radiation heat transfer coefficient from the upper surface of PV/T to the sky can be calculated using Equation 5 [28].

$$h_{rad} = \epsilon_G \sigma (T_{sky} + T_{cell})(T_{sky}^2 + T_{cell}^2) \quad (5)$$

Sky temperature is calculated using Equation 6 [30].

$$T_{sky} = 0.0552 \times T_{amb}^{1.5} + 2.625 \times N \quad (6)$$

Also, the thermal capacity of Tedlar film is ignored. The energy balance for the bottom layer of Tedlar can be calculated from Equation 7 [25, 28].

$$U_T(T_{cell} - T_{bs})bdx = h_f(T_{bs} - T_f)bdx \quad (7)$$

h_f is convection heat transfer in the flow duct, it is calculated according to the flow regime and the Nusselt number of the flow (Equation 8).

$$h_f(T_{bs} - T_f)bdx = m \cdot C_p(dT_f/dx)dx + U_b(T_f - T_{amb})bdx \quad (8)$$

The fluid flow rate can be calculated using Equation 9 [26, 28].

$$m \cdot C_p = \rho V_{in}(b\delta) \quad (9)$$

The overall heat transfer coefficient from the bottom of the PV/T to the environment through the underlying insulation (U_b) is calculated using Equation 10.

$$U_b = [L_i/K_i + 1/h_{conv,b}]^{-1} \quad (10)$$

The surface temperature of the solar photovoltaic module and the temperature of the subsurface layer are obtained as Equations 11 and 12, respectively [26, 28].

$$T_{cell} = \frac{(\alpha\tau)_{eff}G + U_t T_{amb} + U_T T_{bs}}{U_t + U_T} \quad (11)$$

$$T_{bs} = \frac{h_{p1}(\alpha\tau)G + U_{tT}T_{amb} + h_f T_f}{U_{tT} + h_f} \quad (12)$$

Which in these equations:

$$(\alpha\tau)_{eff} = \tau_G[\alpha_c \beta_c + \alpha_r(1 - \beta_c) - \beta_c \eta_{e1}] \quad (13)$$

$$h_{p1} = U_T/(U_T + U_t) \quad (14)$$

$$U_{tT} = [1/U_t + 1/U_T]^{-1} = U_t U_T/(U_T + U_t) \quad (15)$$

By placing Equation (12) in Equation (8), a typical differential equation for fluid temperature in the flow duct is obtained with Equation 16:

$$\frac{dT_f}{dx} + \left(\frac{bU_L}{m \& C_p}\right)(T_f - T_{amb}) = \frac{bh_{p1}h_{p2}(\alpha\tau)_{eff}G}{m \& C_p} \quad (16)$$

In these equations [1, 28]:

$$h_{p2} = h_f/(U_{tT} + h_f) \quad (17)$$

$$U_{tT} = [1/h_f + 1/U_{tT}]^{-1} = U_{tT}h_f/(U_{tT} + h_f) \quad (18)$$

$$U_L = U_b + U_{tT} \quad (19)$$

The overall heat dissipation coefficient has been considered constant in previous research; however, it is not constant and is obtained by modeling the heat and radiative transfer between PV/T surfaces and the environment. The temperature distribution of the fluid according to the length of the flow duct is obtained as Equation 20 [1, 2]:

$$T_f(x) = \left(T_{amb} + \frac{h_{p1}h_{p2}(\alpha\tau)_{eff}G}{U_L}\right) \left(1 - \exp\left(\frac{-bU_L x}{m \& C_p}\right)\right) + T_{f,in} \exp\left(\frac{-bU_L x}{m \& C_p}\right) \quad (20)$$

Applying equation 20 to $x=L$ we obtain the temperature of the fluid leaving the PV/T device; therefore, the temperature of the fluid leaving PV/T as Equations 21:

$$T_{f,out} = \left(T_{amb} + \frac{h_{p1}h_{p2}(\alpha\tau)_{eff}G}{U_L}\right) \left(1 - \exp\left(\frac{-bU_L L}{m \& C_p}\right)\right) + T_{f,in} \exp\left(\frac{-bU_L L}{m \& C_p}\right) \quad (21)$$

The average temperature of the operating fluid in the flow channel is calculated as Equation 22:

$$\bar{T}_f = \frac{1}{L} \int_{x=0}^L T_f(x) dx = \left[T_{amb} + \frac{h_{p1}h_{p2}(\alpha\tau)_{eff}G}{U_L} \right] * \left[1 - \frac{\left(1 - \exp\left(\frac{-bU_L L}{m \cdot C_p}\right) \right)}{\left(\frac{bU_L L}{m \cdot C_p}\right)} \right] + \left[1 - \exp\left(\frac{-bU_L L}{m \cdot C_p}\right) \right] \quad (22)$$

The useful heat rate absorbed in PV/T is calculated from Equations 23 and 24:

$$Qu = \frac{m \cdot C_p}{U_L} [h_{p1}h_{p2}(\alpha\tau)_{eff}G - U_L(T_{f,in} - T_{amb})] * \left[1 - \exp\left(\frac{-bU_L L}{m \cdot C_p}\right) \right] \quad (23)$$

PV/T thermal efficiency is defined as follows:

$$\eta_{th} = \frac{Qu}{bLG} = \frac{m \cdot C_p}{bLU_L} \left[h_{p1}h_{p2}(\alpha\tau)_{eff} - \frac{U_L(T_{f,in} - T_{amb})}{G} \right] * \left[1 - \exp\left(\frac{-bU_L L}{m \cdot C_p}\right) \right] \quad (24)$$

C) Electrical analysis

The appearance of the electrical efficiency parameter (η_{el}) in Equation (25) makes PV/T thermal analysis dependent on the electrical analysis of the photovoltaic module. In previous research, the electrical efficiency has been calculated from Equation 25 [14]:

$$\eta_{el} = \eta_{el,ref} [1 - 0.0045(T_{cell} - T_{amb,ref})] \quad (25)$$

Equation (25) is a linear function of the surface temperature of the solar photovoltaic module and does not detail the changes in electrical parameters such as open circuit voltage, short circuit current, voltage and current at the maximum power point, and so on. However, in this study, the electrical efficiency is calculated from the simulation of a solar photovoltaic module, which can predict changes in electrical parameters relative to changes in functional, environmental, and design parameters. The following transfer Equations 26-34 are used to obtain voltage and current at temperature and other radiation intensities [21-24]:

$$T_{cell} = T_{amb} + G(NOCT - 293.15)/800 \quad (26)$$

$$a/a_{ref} = T_{cell}/T_{cell,ref} \quad (27)$$

$$\frac{I_o}{I_{o,ref}} = \left(\frac{T_{cell}}{T_{cell,ref}} \right)^3 \exp \left(\frac{\varepsilon N_c}{a_{ref}} \left(1 - \frac{T_{cell,ref}}{T_{cell}} \right) \right) I_L \quad (28)$$

$$I_L = G/G_{ref} [I_{L,ref} + \alpha(T_{cell} - T_{cell,ref})] \quad (29)$$

$$\Delta T = T_{cell} - T_{cell,ref} \quad (30)$$

$$\Delta I = \alpha \left(\frac{G}{G_{ref}} \right) \Delta T + \left(\frac{G}{G_{ref}} - 1 \right) I_{se,ref} \quad (31)$$

$$\Delta V = \beta \Delta T - R_s - R_s \Delta I \quad (32)$$

$$I_{new} = I_{ref} + \Delta I \quad (33)$$

$$V_{new} = V_{ref} + \Delta V \quad (34)$$

Silicon has a band gap of 1.12 eV (electron volt). Values of N_c , $NOCT$, β , and α are given by the manufacturers of solar modules. The new values of voltage and current at the maximum power point are obtained from the maximum area of the rectangle below the characteristic curve under the new conditions. The electrical efficiency of a solar photovoltaic array can be calculated by Equations 35 and 36 [14, 17].

$$\eta_{el} = V_{mp} I_{mp} / S_{eff} \quad (35)$$

$$S_{eff} = (N_s N_m A_{mod}) G = A_{arr} G \quad (36)$$

The overall efficiency of the PV/T system is defined as Equation 37 [17, 18]:

$$\eta_{ov} = \frac{\eta_{el}}{0.36} + \eta_{th} \quad (37)$$

D) Optimization study

The first step in the optimization problem is the definition of the objective function proportional to the specific objectives, in other words, the objective function is the design criterion. Sometimes there are several goals in optimization instead of one goal, such issues are called multi-objective optimization. Since single-objective problem optimization has a higher accuracy and is much simpler than multi-objective problems if possible, the one-objective method is used in optimizations. In this research, due to the importance of high accuracy, a single-purpose method has been used. In this research, the objective function includes electrical and thermal efficiencies that the geometric constraints of the studied system are considered as constraints of the objective function. The objective function of the research can be considered as maximizing efficiency or minimizing costs.

3. Results

Figures 3 to 7 show the values of the modelling results for the study area. Figure 3 shows the temperature of the output fluid from the PVT system, according to which the highest output temperature is related to midnight with a value of 61.5 °C and the lowest temperature is related to the

initial hour with a value of 40 °C. According to the outlet temperatures of the fluid, it can be said that these values are suitable for water heating and this system can also be used for water heating of the building.

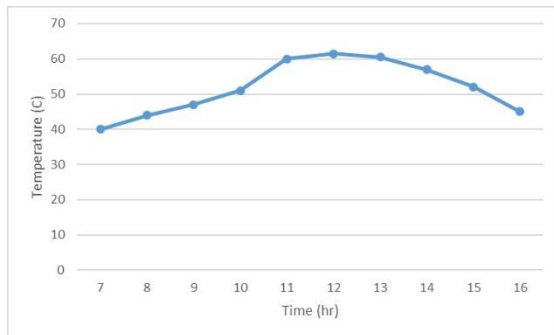


Fig. 3. Temperature values of the output fluid from the PVT system for different hours with an inlet temperature of 25 °C

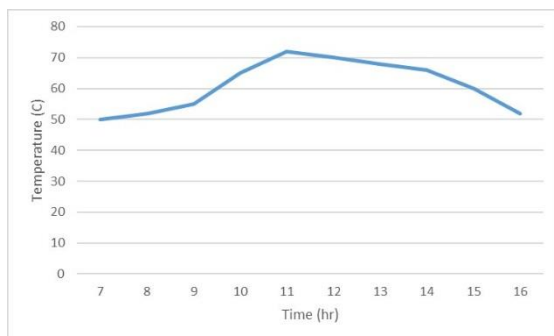


Fig. 4. Photovoltaic cell temperature values for different hours (1000 W/m²)

Figure 4 shows the temperature of the photovoltaic cell (with a standard temperature of 25 °C), according to which the highest temperature of the cell surface is related to midnight with a value of 72 °C and the lowest temperature is related to the initial hour with a value of 50 °C. According to the extraction temperature, it can be seen that to prevent the decrease in efficiency due to the increase in temperature of the cell surface, a cooling system should be used so that the efficiency of the system works in an acceptable range.

According to Figure 5, it can be seen that the maximum voltage and current are related to 8 and 12 hours, respectively, for which the amount of voltage is 20 V and the amount of current is 7.5 A. According to previous findings, the amount of electrical and thermal efficiency for the PVT system for different radiation intensities can be seen in Figure 6.

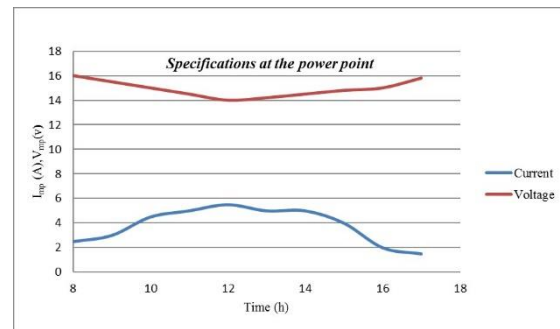


Fig. 5. Simulation results for voltage and current at different times

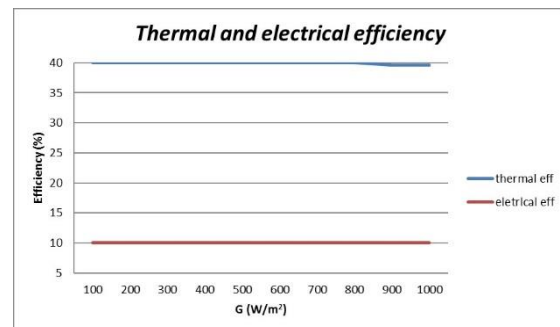


Fig. 6. Changes in thermal and electrical efficiency in terms of solar radiation intensity

As shown in Figure 6, as the intensity of the sun's rays increases, the overall and electrical efficiencies first increase and then decrease, but the thermal efficiencies decrease, although this decrease is not as severe. On the other hand, to have the minimum general, thermal and electrical efficiencies for the PV/T system, there must be a minimum intensity of solar radiation. The maximum intensity of solar radiation due to the increase of pollutants in the atmosphere reaches about 1000 W/m². However, determining the intensity of solar radiation is not in our hands and is related to the geographical location and radiation data of that geographical location, but what is clear is that the design of the PV/T system should be based on the average daily or monthly average solar intensity. As can be seen in Figure 6, it shows the electrical and thermal efficiency for different radiation intensity, which with the increase solar radiation, the electrical efficiency is constant and 10% around but the thermal efficiency has a constant value of 40% up to 800W/m² radiation, and after that the thermal efficiency decreases with the increase of radiation intensity, so that for 1000 W/m² radiation, the thermal efficiency is 39%. Accordingly, the amount of electrical and thermal efficiencies for the study area will be according to Figure 7.

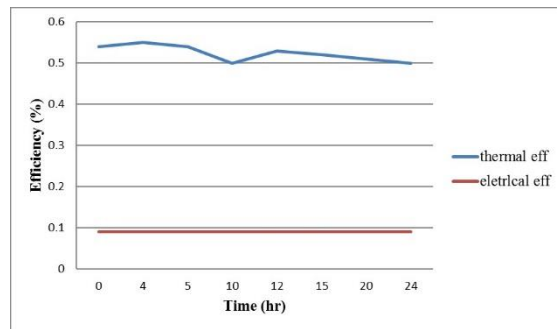


Fig. 7. Electrical and thermal efficiencies for the PVT system per hour

As can be seen in Figure 7, it shows the electrical and thermal efficiency for 24 hours, which with the passage of time, the electrical efficiency is constant and around 9%, and the thermal efficiency decreases with the passage of time, so that the maximum efficiency is equal to 54%. Two independent parameters for optimized inlet flow velocity and PV/T surface area to maximize the overall efficiency equation are found in Table 2:

$V_{in,opt} = 10 \text{ m/s}$	$\eta_{ov,max} = 67\%$
$A_{c,opt} = 2.5296 \text{ m}^2$	

4. Conclusion

In this research, comprehensive mathematical modelling of PV/T thermal and electrical operating conditions was performed. Then, the overall efficiency of PV/T was obtained and a comparison was made with the previous works. Finally, by MATLAB software optimization functions, the overall efficiency of PV/T in a set of certain environmental conditions was optimized for some functional and design parameters such as fluid inlet temperature, PV/T surface area, etc., and the optimal values of these parameters and related parameters were obtained. The effect of other parameters that were assumed to be constant during optimization on overall thermal and electrical efficiencies was also investigated. In addition to increasing the accuracy of the results, the optimal operation mode of PV/T has been achieved, and also the results show that the effect of design parameters such as PV/T surface area on overall efficiency is less than functional parameters such as inlet fluid velocity, inlet fluid temperature and so on. Research that can be done in the future:

- Numerical and experimental investigation combined heat and power with PVT system.
- Exergo-economic analysis of PVT system.

Nomenclature

A_{arr}	Surface area of PV array (m^2)
A_{mod}	Surface area of PV panel (m^2)
b	Collector width (m)
$b\delta$	Flow duct cross-section (m^2)
C_p	Heat capacity of fluid (J/kg. $^{\circ}\text{C}$)
G	Solar radiation (W/m^2)
$h_{conv.b}$	Displacement heat transfer coefficient at the bottom of PV/T ($\text{W}/\text{m}^2. ^{\circ}\text{C}$)
$h_{conv.t}$	The heat transfer coefficient of displacement from the upper surface of PV/T to the environment ($\text{W}/\text{m}^2. ^{\circ}\text{C}$)
h_f	Convection heat transfer in the flow duct ($\text{W}/\text{m}^2. ^{\circ}\text{C}$)
h_{rad}	Radiation heat transfer coefficient from the upper surface of PV/T to the sky ($\text{W}/\text{m}^4. ^{\circ}\text{K}^4$)
K_i	Insulation conductivity coefficient ($\text{W}/\text{m}^2. ^{\circ}\text{C}$)
K_G	Coefficient of conductivity of glass
K_T	Subsurface layer coefficient ($\text{W}/\text{m}^2. ^{\circ}\text{C}$)
L	Flow duct length (m)
L_G	Thickness of glass (m)
L_i	Insulation thickness (m)
L_T	Subsurface layer Thickness (m)
\dot{m}	Fluid flow rate (kg/s)
N	Sky cloud coverage in octaves
$NOCT$	Nominal Operating Cell Temperature ($^{\circ}\text{C}$)
N_c	Number of cells
N_m	Number of panels in a string
N_s	Number of strings
S_{eff}	Effective solar radiation (W/m^2)
T_{amb}	Ambient temperature ($^{\circ}\text{C}$)
T_{cell}	Solar cell temperature ($^{\circ}\text{C}$)
T_{bs}	Temperature of the back surface layer ($^{\circ}\text{C}$)
T_f	The temperature of the fluid inside the flow duct ($^{\circ}\text{C}$)
T_{sky}	Sky temperature ($^{\circ}\text{C}$)
U_b	The overall heat transfer coefficient from the bottom of the PV/T to the environment through the underlying insulation ($\text{W}/\text{m}^2. ^{\circ}\text{C}$)
U_L	Overall heat loss coefficient ($\text{W}/\text{m}^2. ^{\circ}\text{C}$)
U_T	The heat transfer coefficient from the photovoltaic cell to the fluid flow through the subsurface layer ($\text{W}/\text{m}^2. ^{\circ}\text{C}$)
U_t	The total heat transfer coefficient of the solar cell to the environment through PV/T glass coating ($\text{W}/\text{m}^2. ^{\circ}\text{C}$)
V_{in}	Average fluid velocity at PV/T input (m/s)
V_w	Wind speed on an upper surface of PV/T (m/s)
x	Collector length (m)
α	Temperature coefficients of current ($\text{A}/^{\circ}\text{C}$)
α_c	Solar cell absorption coefficient
α_T	Subsurface layer absorption coefficient
β	Temperature coefficients of voltage ($\text{V}/^{\circ}\text{C}$)
β_c	Solar cell density coefficient
ε	Band gap energy (eV)
ε_G	Glass issuance coefficient ($\text{W}/\text{m}^2. ^{\circ}\text{C}$)
η_{ov}	Overall efficiency (%)
η_{el}	Electrical efficiency (%)
σ	Stefan-Boltzman coefficient ($\text{W}/\text{m}^2. \text{K}^4$)
τ_G	Glass transfer coefficient ($\text{W}/\text{m}^2. ^{\circ}\text{C}$)

References

- [1] Joshi, S. S., & Dhoble, A. S. (2018). Photovoltaic-Thermal systems (PVT): Technology review and future trends. Renewable and Sustainable Energy Reviews, 92, 848-882.
- [2] Hamzat, A. K., Sahin, A. Z., Omissanya, M. I., & Alhems, L. M. (2021). Advances in PV and PVT cooling technologies: A review. Sustainable Energy Technologies and Assessments, 47, 101360.
- [3] Vahdatpour, S., Behzadfar, S., Siampour, L., Veisi, E., & Jahangiri, M. (2017). Evaluation of off-grid hybrid renewable systems in the four climate regions of Iran. Journal of Renewable Energy and Environment, 4(1), 61-70.

- [4] Jahangiri, M., Karimi Shahmarvandi, F., & Alayi, R. (2021). Renewable energy-based systems on a residential scale in southern coastal areas of Iran: trigeneration of heat, power, and hydrogen. *Journal of Renewable Energy and Environment*, 8(4), 67-76.
- [5] Jahangiri, M., & Shamsabadi, A. A. (2017). Designing a horizontal-axis wind turbine for South Khorasan province: A case study. *International Journal of Precision Engineering and Manufacturing*, 18, 1463-1473.
- [6] Alayi, R., Khan, M. B., & Mohammadi, M. S. G. (2020). Feasibility study of grid-connected PV system for peak demand reduction of a residential building in Tehran, Iran. *Mathematical Modelling of Engineering Problems*, 7(4), 563-567.
- [7] Çiftçi, E., Khanlari, A., Sözen, A., Aytaç, İ., & Tuncer, A. D. (2021). Energy and exergy analysis of a photovoltaic thermal (PVT) system used in solar dryer: A numerical and experimental investigation. *Renewable Energy*, 180, 410-423.
- [8] Fu, Z., Li, Y., Liang, X., Lou, S., Qiu, Z., Cheng, Z., & Zhu, Q. (2021). Experimental investigation on the enhanced performance of a solar PVT system using micro-encapsulated PCMs. *Energy*, 228, 120509.
- [9] AlMallahi, M. N., El Haj Assad, M., AlShihabi, S., & Alayi, R. (2022). Multi-criteria decision-making approach for the selection of cleaning method of solar PV panels in United Arab Emirates based on sustainability perspective. *International Journal of Low-Carbon Technologies*, 17, 380-393.
- [10] Alayi, R., Khalilpoor, N., Heshmati, S., Najafi, A., & Issakhov, A. (2021). Thermal and environmental analysis solar water heater system for residential buildings. *International Journal of Photoenergy*, 2021, 1-9.
- [11] Fu, Z., Liang, X., Li, Y., Li, L., & Zhu, Q. (2021). Performance improvement of a PVT system using a multilayer structural heat exchanger with PCMs. *Renewable Energy*, 169, 308-317.
- [12] Fudholi, A., Zohri, M., Rukman, N. S. B., Nazri, N. S., Mustapha, M., Yen, C. H., ... & Sopian, K. (2019). Exergy and sustainability index of photovoltaic thermal (PVT) air collector: A theoretical and experimental study. *Renewable and Sustainable Energy Reviews*, 100, 44-51.
- [13] Sun, Q., Lin, D., Khayatnezhad, M., & Taghavi, M. (2021). Investigation of phosphoric acid fuel cell, linear Fresnel solar reflector and Organic Rankine Cycle polygeneration energy system in different climatic conditions. *Process Safety and Environmental Protection*, 147, 993-1008.
- [14] Fayaz, H., Rahim, N. A., Hasanuzzaman, M., Nasrin, R., & Rivai, A. (2019). Numerical and experimental investigation of the effect of operating conditions on performance of PVT and PVT-PCM. *Renewable Energy*, 143, 827-841.
- [15] Xu, Y. P., Ouyang, P., Xing, S. M., Qi, L. Y., & Jafari, H. (2021). Optimal structure design of a PV/FC HRES using amended Water Strider Algorithm. *Energy Reports*, 7, 2057-2067.
- [16] Verma, A. H., Joshi, S. K., Singh, Y. K., & Dubey, S. (2021). A neural network model of PV module temperature as a function of weather parameters prevailing in composite climate zone of India. *International Journal of Ambient Energy*, 1-5.
- [17] Abdul-Ganiyu, S., Quansah, D. A., Ramde, E. W., Seidu, R., & Adaramola, M. S. (2021). Study effect of flow rate on flat-plate water-based photovoltaic-thermal (PVT) system performance by analytical technique. *Journal of Cleaner Production*, 321, 128985.
- [18] Saadon, S., Gaillard, L., Menezes, C., & Giroux-Julien, S. (2020). Exergy, exergoeconomic and enviroeconomic analysis of a building integrated semi-transparent photovoltaic/thermal (BISTPV/T) by natural ventilation. *Renewable Energy*, 150, 981-989.
- [19] Alayi, R., Harasii, H., & Pourderogar, H. (2021). Modeling and optimization of photovoltaic cells with GA algorithm. *Journal of Robotics and Control (JRC)*, 2(1), 35-41.
- [20] Jermsittiparsert, K. (2021). Examining the sustainable energy and carbon emission on the economy: panel evidence from ASEAN. *International Journal of Economics and Finance Studies*, 13(1), 405-426.
- [21] Gao, Y., Hu, G., Zhang, Y., & Zhang, X. (2022). An experimental study of a hybrid photovoltaic thermal system based on ethanol phase change self-circulation technology: Energy and exergy analysis. *Energy*, 238, 121663.
- [22] Al-Waeli, A. H., Sopian, K., Yousif, J. H., Kazem, H. A., Boland, J., & Chaichan, M. T. (2019). Artificial neural network modeling and analysis of photovoltaic/thermal system based on the experimental study. *Energy Conversion and Management*, 186, 368-379.
- [23] Sridharan, M., & Jayaprakash, G. (2019). Verification and validation of solar photovoltaic thermal water collectors performance using fuzzy logic. *Journal of Verification, Validation and Uncertainty Quantification*, 4(4).
- [24] Daghigh, R., Ruslan, M. H., & Sopian, K. (2011). Advances in liquid based photovoltaic/thermal (PV/T) collectors. *Renewable and Sustainable Energy Reviews*, 15(8), 4156-4170.
- [25] Shahsavari, A., Ameri, M., & Mahmoud Abadi, M. M. (2011). Simulation and test of pv/t air systems with natural air flow operation. *Amirkabir Journal of Mechanical Engineering*, 43(1), 31-40.
- [26] Joshi, A. S., & Tiwari, A. (2007). Energy and exergy efficiencies of a hybrid photovoltaic-thermal (PV/T) air collector. *Renewable Energy*, 32(13), 2223-2241.
- [27] Bhattarai, S., Oh, J. H., Euh, S. H., Kafle, G. K., & Kim, D. H. (2012). Simulation and model validation of sheet and tube type photovoltaic thermal solar system and conventional solar collecting system in transient states. *Solar Energy Materials and Solar Cells*, 103, 184-193.
- [28] Yazdanifard, F., Ebrahimnia-Bajestan, E., & Ameri, M. (2016). Investigating the performance of a water-based photovoltaic/thermal (PV/T) collector in laminar and turbulent flow regime. *Renewable Energy*, 99, 295-306.
- [29] Herrando, M., Pantaleo, A. M., Wang, K., & Markides, C. N. (2019). Solar combined cooling, heating and power systems based on hybrid PVT, PV or solar-thermal collectors for building applications. *Renewable Energy*, 143, 637-647.
- [30] Aste, N., Chiesa, G., & Verri, F. (2008). Design, development and performance monitoring of a photovoltaic-thermal (PVT) air collector. *Renewable energy*, 33(5), 914-927.